Journal of Harbin Engineering University
ISSN: 1006-7043
Vol 46 No. 4
April 2025

Ligand-Guided Homology Modelling of the Human Bitter Taste Receptor TAS2R10

Arati Prabhu[a*#], Bandoo Chatale[b,c], Mariam S. Degani[b*#]

[a]*SVKM's Dr. Bhanuben Nanavati College of Pharmacy, Mumbai, India*

[b]*Department of Pharmaceutical Sciences &Technology Institute of chemical technology, Mumbai 400019, India*

[c]*Present address - Department of Pharmaceutical Chemistry, Mumbai Educational Trust Institute of Pharmacy, Mumbai, India*

[#]*Arati Prabhu and Mariam S. Degani should be considered jointly as joint senior authors*

Abstract

Despite low sequence identity with crystallized GPCRs, a homology model of the bitter receptor, TAS2R10 was constructed using single-template comparative modeling and refined using a combination of docking and molecular dynamic simulations. This ligand-guided strategy for model refinement resulted in an excellent correlation between the binding affinity of a chemically diverse set of known TAS2R10 bitter ligands and their docking scores with a r^2 value of 0.87, giving credence to the accuracy of the built homology model. A critical analysis of the binding site interactions of the bitter ligands revealed the all-encompassing nature of the TAS2R10 active site with a balanced blend of both polar as well as hydrophobic amino acids, bestowing it with promiscuity towards a large set of diverse bitter ligands. This functionally validated homology model can be used for the structure-based screening of compounds for their bitter tasting potential.

Keywords: TAS2R10; Human Bitter Taste Receptor; Homology modelling, Ligand-guided, Molecular Dynamic Simulations

1. Introduction

The development of oral formulations of bitter drugs presents formidable challenges to the pharmaceutical scientist from the context of palatability and patient compliance. Although, the perception of bitter taste helps to protect organisms from ingestion of toxic substances[1], [2] there are innumerable examples of bitter compounds with significant therapeutic activity[3]. Bitterness of compounds is mediated by a small subclass of taste receptors encoded by the taste 2 receptor (TAS2R) genes[4]–[6]. The human TAS2R progenitors consist of twenty-five functional proteins, which belong to the superfamily of G protein-coupled receptors (GPCRs)[7], [8]. The bitter taste receptors can perceive a large number of chemically diverse substances as bitter. Some examples are peptides and hydroxyl fatty acids, functional groups such as esters, amines, amides, thioureas, azacycloalkanes, lactones, N-heterocyclic compounds, carbamides, carbonyl compounds, phenols, crown ethers as well as natural products such as alkaloids,

glycosides, terpenoids, flavonoids, steroids, halogenated or acetylated sugars and metal ions[9], [10]. Of the twenty-five receptor structures which have been identified for bitter taste, TAS2R10 [11], TAS2R14 [12]and TAS2R46 [13] have been identified as receptors for most of the in-vitro tested bitter compounds to date [14].

Several methods such as phylogenetic-like tree construction, quantitative nuclear magnetic resonance, and ligand identification have been used to identify the structural components responsible for bitter taste in molecules [15]–[17]. Chemical modification of these structural features may dramatically reduce the bitter taste, but carry the risk of tampering with the pharmacological activity of the compounds. Structure-based drug modulation offers a rational way to design analogues of bitter drugs with decreased affinity for the TAS2R bitter receptors, which however can retain their primary therapeutic activity. Targeted designing of non-bitter analogues of medicinally beneficial drugs necessitates the availability of the three-dimensional structures of the taste receptors. However, the G protein-coupled taste receptors have not yet been elucidated by X-ray crystallography or NMR spectroscopy.

As a way forward, we have constructed the homology model of TAS2R10 receptor using single-template knowledge-based homology modelling and refined it by a combination of techniques such as long molecular dynamics simulations (MDS) and induced fit docking (IFD) of known TAS2R10 bitter ligands.

2. Methodology

2.1. Homology Modelling

Homology model of TAS2R10 was built using the Prime module[b] of Schrodinger. The protein sequence of TAS2R10 receptor protein was retrieved from Uniprot Knowledgebase database[18] using accession no. Q9NYW0. BLASTp search within the Protein Data Bank (PDB) was used to find templates with best sequence identity with TAS2R10. The crystal structure of the β2 adrenergic receptor G-protein complex (GPCRs in agonist-bound active conformations) was selected as template (PDB code: 3SN6) and was downloaded from the PDB. The sequence alignment of TAS2R10 with 3SN6 was performed using Prime STA (best for low sequence identity) using the GPCR-specific alignment modality. The secondary structure of TAS2R10 was imported from the PSIPRED server (bioinf.cs.ucl.ac.uk/psipred). The homology model of human TAS2R10 was built with the PRIME module[b] of Schrödinger suite using the knowledge-based modelling protocol. The homology model was subjected to various refinement protocols such as optimization of side-chains and refinement of loops. Subsequently, the entire structure was energy-minimised using a truncated-Newton energy minimization protocol. The OPLS_2005 all-atom force field was used and solvation energies were treated via the Surface Generalized Born (SGB) continuum solvation model.

2.2. Structure refinement of homology model by MD simulations

The homology model of TAS2R10 was subjected to a lengthy MDS run for structure stabilization. The apo structure was soaked in a simulation box along with 21,105 SPC water molecules under orthorhombic boundary conditions in the System Builder panel of the Desmond[d] module of Schrodinger. 100 ns molecular dynamics (MD) simulation was performed and then run on the relaxed systems with a NPT ensemble using a Berendsen thermostat at 300 K.

2.3. Structural validation

The geometry of the constructed TAS2R10 structure was assessed by inspection of all the phi/psi torsions and fit of their distributions within the Ramachandran plot obtained through PROCHECK analysis [19]. The model was further analysed using ProSA-web, an interactive web service which assesses structural errors in protein models and assigns Z-scores that indicates the overall quality of the model. [20], [21]

2.3. Active Site prediction

The Site Map module[e] from Schrodinger was used to characterize the binding pockets and functional residues of the optimized protein structure of TAS2R10. Site Map uses grid points to identify regions on the protein surface that may be suitable for binding ligands to the receptor[22].

2.4. Selection of reference bitter ligand for ligand-guided model optimization

Compounds which are known to be bitter by virtue of binding to TAS2R10 were downloaded from the BitterDB database available at http://bitterdb.agri.huji.ac.il/bitterdb[3]. This database includes 1041 compounds binding to all the bitter receptors that have been documented as bitter-tasting to humans. The compounds can be filtered in accordance with various criteria, including their association with particular human bitter taste receptors. The most active TAS2R10 bitter ligand cucurbitacin E was selected for ligand-guided refinement of the TAS2R10 structure on the basis of its binding affinity to TAS2R10.

2.5. Ligand preparation

The ligand 3D structure was generated using the Ligprep module[a] of Schrodinger using the OPLS2005 force field to produce one low energy ring conformation per ligand.

2.6. Induced fit Docking (IFD) of a known reference bitter compound

The Induced Fit Docking module[f] (IFD) of Schrodinger software was used to dock the standard bitter ligand inside the binding pocket of TAS2R10 receptor. The Induced Fit Docking (IFD) protocol uses grid scoring, hierarchical filtering to accurately predict ligand binding modes, while performing a refinement on the protein that documents concomitant structural changes in the receptor.

2.7. Structure refinement of docked complexes by MD simulations

The molecular dynamics simulations of the docked complex of the selected bitter ligand, cucurbitacin E was performed using the Desmond module.[e] In order to mimic the membrane bound environment of the GPCR receptors, the ligand-TAS2R10

complex was embedded in a water–lipid box using System Builder and neutralized with chloride ions. The input protein complex was aligned to a pre-equilibrated protein-membrane system. The boundary box size was calculated using the default buffer distance of 10Å. The resulting system had 68 lipid molecules and14 chloride ions. All atom 1-palmitoyl-2-oleoylphosphatidylcholine bilayer (POPC) and SPC water were used for the lipid and water models respectively[23]. The size of system was 35,000 atoms. The default protocol integral to Desmond was used for the simulation. The backbone torsions were however constrained and the whole system was subjected to a series of restrained minimizations and molecular dynamics simulations, thereby ensuring that the system slowly relaxes without deviating considerably from the initial protein coordinates[24]. The simulation was performed under periodic boundary conditions at a constant temperature maintained by Nose-Hoover thermostats, while the Martyna–Tobias–Klein method was used to control the pressure. The multi-step RESPA integrator with an inner time step of 2.0 fs for bonded interactions was used for integrating the equations of motion. Non-bonded interactions were integrated within the short-range cut-off and an outer time step of 6.0 fs as applied beyond the cut-off. Prior to the MD simulations, 2,000 steps of minimization with the steepest descent method were used to remove high-energy interatomic contacts [25]. Molecular dynamics simulations were then run for 80 ns on the relaxed systems with a NPT ensemble using a Berendsen thermostat at 300 K and the trajectory was recorded after every 4.8 ps.

2.8. **Validation molecules from BitterDB**

Forty-five TAS2R10 ligands are compiled in the BitterDB[26] to date, of which the EC_{50} values have been reported for twenty-five bitter compounds. These chemically and therapeutically diverse bitter ligands with TAS2R10 EC_{50} ranging from 0.01 μM to 10000 μM were shortlisted for the docking. The 3D conformer of the ligand molecules was downloaded from the Pubchem database[27]in sdf format and converted to pdb file format using Open Babel software[28].

2.9. **Docking of validation set of bitter ligands**

Docking-based virtual screening of the twenty-five known bitter ligands was used to validate the structural accuracy of the constructed homology model. Autodock Vina 1.1.2 was used to perform the docking exercise within the open-source PyRx 0.8 software[29]. The bitter ligand molecules were energy minimized with the universal forcefield (UFF) using the conjugate gradient optimization algorithm to an energy convergence of 0.01 kcal/mol and converted to the required pdbqt file format within PyRx. The grid box was centred at (-6.6154, -6.9503, 3.3694) coordinates of the TAS2R10 protein and had dimensions of (22.5, 22.5, 22.75) $Å^3$ to adequately cover the selected binding site. The docking runs were made with an exhaustiveness parameter of 8 and the top-ranking complexes of each ligand were

analysed in the BIOVIA Discovery Studio Visualizer[30]

3. Results and Discussion

3.1. Homology Modelling

Agonist-bound conformation of the template protein β2 adrenergic receptor, 3SN6 was used to build the activated form of the bitter receptor. This was thought to facilitate the subsequent docking of bitter ligands which would need the open active site for binding. The pair-wise comparison of TAS2R10 with the experimentally solved GPCR showed 11.63 % sequence identity with the tingle template protein. The sequence alignment between the β2 adrenergic receptor and TAS2R10 is shown in Figure 1.

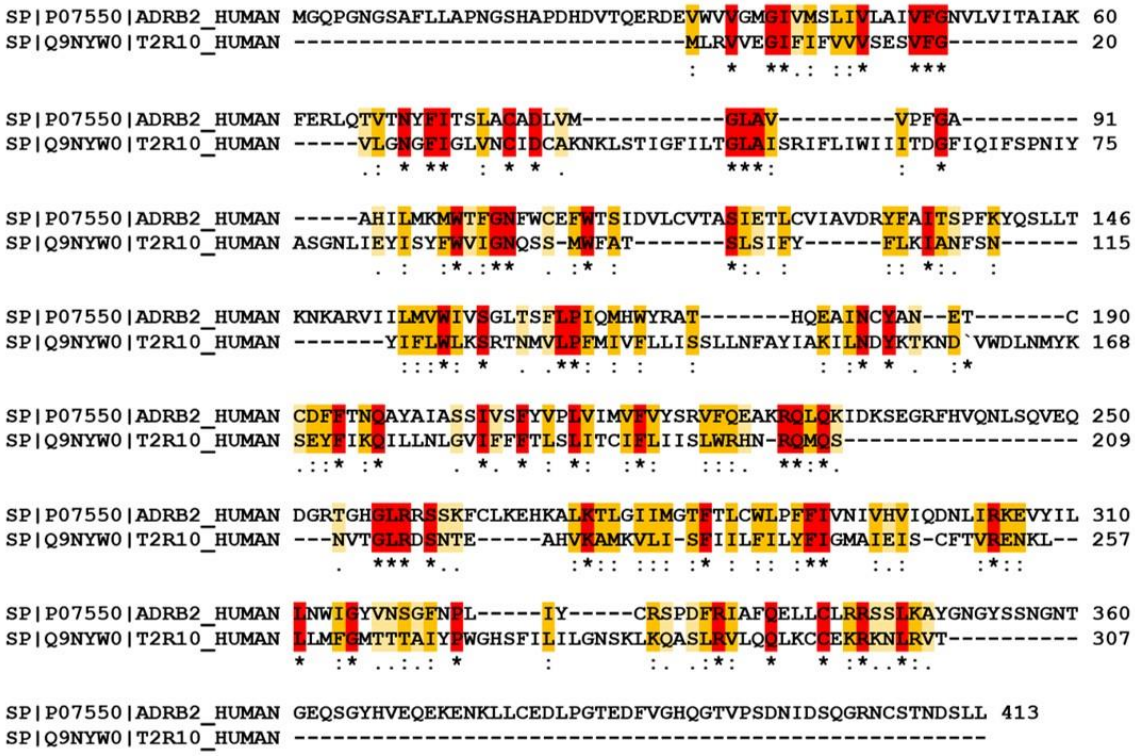

Figure 1: Sequence alignment between the β2 adrenergic receptor and TAS2R10. The sequences have been color-coded on the basis of identity and residue conservation. (* Star sign indicates identical residues and have been marked with red highlights; : colon sign indicates conserved substitutions and have been marked with orange highlights; . period sign indicates semi-conserved substitutions and have been marked with yellow highlights)

Owing to the poor sequence identity between TAS2R10 and the crystallised GPCRs deposited in the PDB, single-template knowledge-based model building coupled with ligand-guided binding site optimization approach was used for building the homology model of TAS2R10 bitter receptor. The theoretical model was built, the positions of the variable loops sampled and the side-chain amino acids optimised with the aid of the in-built rotamer library within Schrodinger software. This was followed by energy minimisation of the entire structure using OPLS2005 all-atom force field until a convergence difference of 0.01 kcal/mol/A

was reached. Structural parameters of the refined model were checked by Ramachandran plot and ProSA-web analysis. The homology model of TAS2R10 and the results of the Ramchandran plot and ProSA-web analysis are shown in Figure 2A, 2B and 2C respectively.

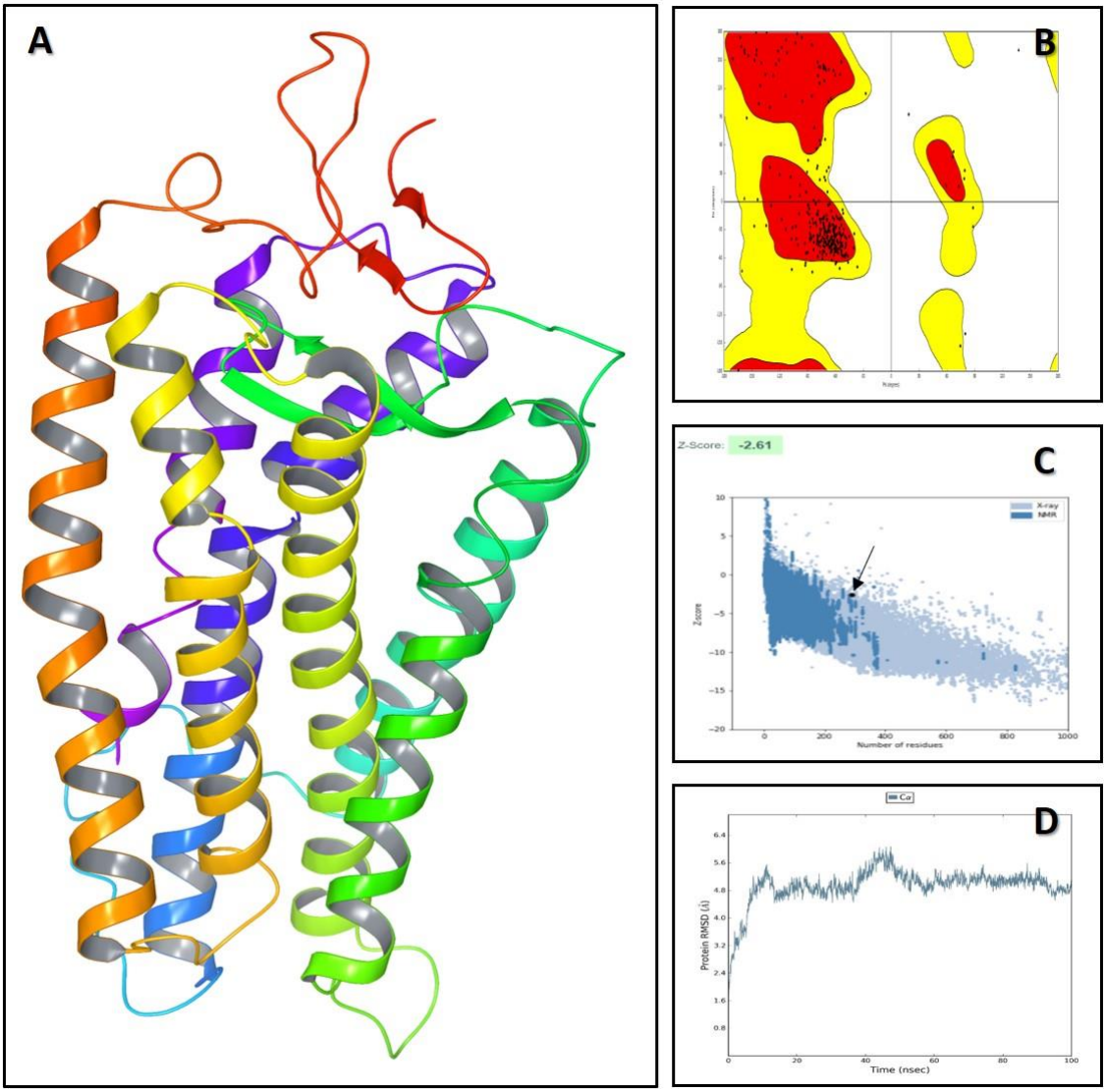

Figure 2:(A) Homology model TAS2R10, (B) Ramachandran plot of TAS2R10 homology model (C) The Z-score of -2.61 (black dot as pointed at by arrow) assigned by ProSA, evaluated according to the ProSA-web algorithm and computed by comparing the model geometry with the chain lengths of all proteins in the PDB elucidated by X-ray diffraction (light blue) and NMR spectroscopy (dark blue), respectively (D) Time evolution of RMSD during 100 ns MDS of membrane-embedded apo structure of TAS2R10

92.5% of the amino acid residues were in the favoured region (red region in Figure 2B) of the Ramchandran plot. Of the remaining, 7.0% were in the allowed region (yellow region in Figure 2B), and 0.5% (white region in Figure 2B) were outliers. The Z-score of TAS2R10 homology model evaluated according to the ProSA-web algorithm was -2.61, which was computed by comparing the model

geometry with the chain lengths of all proteins in the PDB elucidated by X-ray diffraction and NMR spectroscopy. This was in the range of native conformations of crystal structures.

Site No.	Site score	D score
3	1.097	0.991
1	1.084	1.150
2	1.053	1.073
4	0.803	0.799
5	0.694	0.551

4. **Table 1.** Site Map predicted sites for TAS2R10

4.1. MD simulation for structure optimization

The apo structure of the homology model was further refined by subjecting it to 100 ns MD simulations. The overall structure RMSD with respect to the starting structure over the course of the simulations is shown in Figure 2D. The structure coordinates were seen to fluctuate up to almost 60 ns, after which a minimal RMS deviation within 2 Å was recorded, which indicates the conformational stability of the overall TAS2R10.

4.2. ctive Site prediction

The probable binding sites of the receptor were mapped by Site Map[e] and scored in accordance with various criteria such as cavity size, solvent exposure, protein enclosure, balance between hydrophilicity and hydrophobicity and the degree to which a ligand might donate or accept hydrogen bonds (27). Site Map predicted five sites on TAS2R10. Table 1 shows the Site scores and the druggability , D values of the five sites.

Site 3, with the best combination of site score as well as druggability score was selected for further IFD study. This site was found to be well balanced with the capability of accommodating hydrophobic as well as hydrophilic compounds with positive or negative groups.

Born et al. have identified the binding site residues in TAS2R10 in an elegant study comprising site-directed mutagenesis and functional assays[14]. Site Map site 3, which lies near the extracellular loops and dips down into a region covered by transmembrane helices 3, 5, 6 and 7 coincides with this binding site charted out as responsible for the agonist-induced activation of TAS2R10.

4.3. Ligand-guided structure refinement

The most probable bioactive pose of the known standard bitter ligand cucurbitacin E was predicted using the induced fit docking algorithm within the selected

binding site of the homology model of TAS2R10.The docked complex of cucurbitacin E-TAS2R10 was embedded in a membrane-simulating lipid-water box and subjected to long molecular dynamics simulations. The purpose of this exercise was to perturb the ligand-bound homology model, thereby inducing the active site residues to adjust themselves and give an optimized binding to the known bitter ligands. This was thought to be a fitting refinement of the homology model from a mechanistic perspective, yielding a stable set of orientations of the binding cavity amino acid residues that resemble the active ligand-bound conformation of the TAS2R10 active site. The simulations were run for a total of 80 ns, during which 1000 structures were enumerated and saved in the trajectory. The RMSD of the protein coordinates with respect to the starting structure was monitored during the MD simulations.

Figure 3 shows the explicit membrane-embedded Cucurbitacin E-bound complex of TAS2R10 and the RMSD time evolution during its 80 ns simulation.

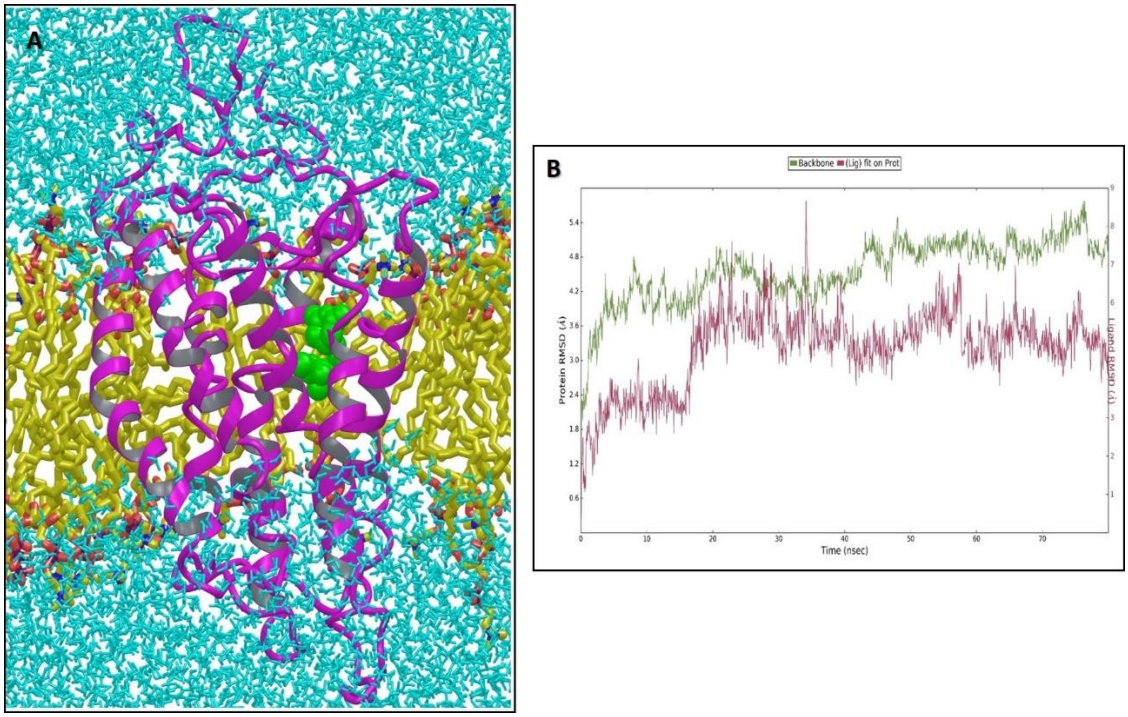

Figure 3: (A) Membrane embedded structure of TAS2R10 (pink ribbons) complexed with Cucurbitacin E (green spheres). The POPC molecules simulating the lipid bilayer membrane are shown as yellow sticks, while the surrounding water is shown as blue lines. (B) - Time evolution of RMSD (green plot – protein coordinates; pink plot – ligand coordinates) during 80ns MDS of membrane-embedded complex of TAS2R10 with Cucurbitacin E.

The Cucurbitacin E -TAS2R10 complex reached RMSD convergence after 20 ns as depicted by the green plot in figure 3B, after which there was minimum fluctuation of 1.5 Å for the protein coordinates. This indicates the conformational stability of the overall bitter ligand-bound TAS2R10 complex. The

structure of the ligand and the nature of its interactions within the active site of TAS2R10 structure showed minor variations within the orientations of the active site residues even after 80 ns molecular dynamics perturbations as is evident from the RMSD fluctuations of 2 Å seen for the ligand (pink plot in figure 3b) after convergence.

4.4. Validation of homology model

4.4.1. Docking of bitter compounds

Twenty-five chemically as well as therapeutically diverse bitter ligands with TAS2R10 EC_{50} ranging from 0.01 M to 10000 M were used as a test set for the validation of the constructed homology model. The docking scores of these ligands along with their EC_{50} values are compiled in Table 2.

Table 2. The docking scores of these ligands along with their EC_{50} values

Figure 4 shows the correlation plot and the correlation equation between the log EC_{50} and

Sr. No.	Pubchem id	Bitter ligand	TAS2R10 EC_{50} (μM)	log EC_{50}	Docking score
1	5281319	cucurbitacin E	0.01	-2.00	-9.4
2	6433476	cucurbitacin B	0.01	-2.00	-9.2
3	19518	denatonium	3	0.48	-8.2
4	441071	strychnine	3	0.48	-8.3
5	8549	quinine	10	1.00	-7.6
6	4680	papaverine	10	1.00	-7.8
7	2725	chlorpheniramine	10	1.00	-7.5
8	8400	benzoin	30	1.48	-7.7
9	6473881	parthenolide	30	1.48	-7.3
10	3055	diphenidol	30	1.48	-7.9
11	11807014	arborescin	100	2.00	-7.5
12	636760	arglabin	100	2.00	-7.6
13	442011	cascarillin	100	2.00	-7.2
14	5959	chloramphenicol	100	2.00	-7.3
15	9649	brucine	100	2.00	-7.3
16	2955	dapsone	100	2.00	-7.5
17	6197	cycloheximide	100	2.00	-7.6
18	4114	Methoxsalen	100	2.00	-7.3
19	221071	(-) o-Santonin	100	2.00	-7.8
20	323	coumarin	300	2.48	-6.8
21	65571	quassin	300	2.48	-6.8
22	2265	azathioprine	300	2.48	-6.5
23	8969	yohimbine	300	2.48	-7.3
24	441095	erythromycin	300	2.48	-7.4
25	2719	chloroquine	10000	4.00	-6.1

the dock scores and of the known TAS2R10 bitter ligands.

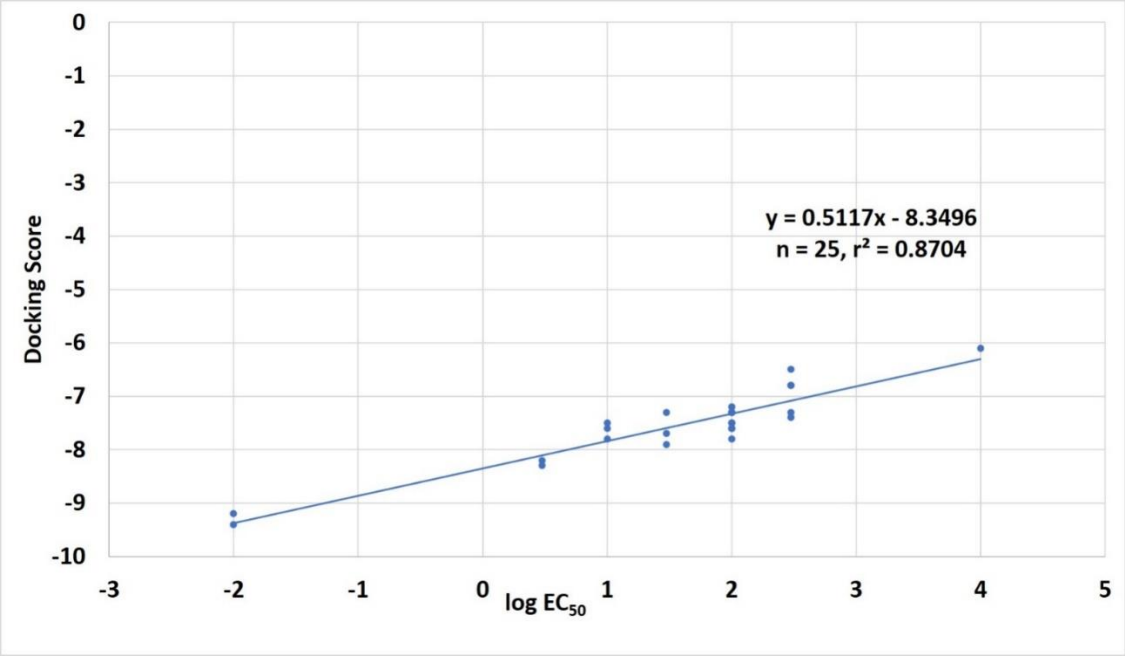

Figure 4: Correlation plot and the correlation equation between the log EC_{50} and the dock scores of the known TAS2R10 bitter ligands

The correlation coefficient of 0.87 attests to the excellent correlation between the experimental binding EC_{50} values and the docking scores of the test set of twenty-five known ligands in the constructed homology model of TAS2R10, thereby providing validation to the structural accuracy of the homology model of TAS2R10.

3.5.2. TAS2R10 bitter motifs

An analysis of the Bitterdb database (3) reveals many interesting facts. Along with TAS2R14 and TAS2R46, TAS2R10 is one of the most promiscuous human bitter receptors known. Compounds with diverse functionalities and topologies exhibit moderate to excellent binding potential to TAS2R10, with the binding potency EC_{50} values ranging from 0.01 µM to 10000 µM. Table 3 enlists the binding interactions of the top-ranked docked poses of the TAS2R10 bitter ligands.

Table 3. The binding interactions of the top-ranked docked poses of the TAS2R10 bitter ligands.

Sr. No.	Bitter ligand	TAS2R10 EC_{50}(µM)	Docking score	Binding site interactions		
				H-bonding	π-stacking	Hydrophobic interactions
1	cucurbitacin E	0.01	-9.4	N92, Y239, K256	L57 I61 I62 K168 F236 P270	-
2	cucurbitacin B	0.01	-9.2	N92, Y239, K256	L57 I62 F236 P270	-
3	denatonium	3	-8.2	W88	F66, F236	W88, Y239, M243, I62
4	strychnine	3	-8.3	-	W88, W88 (NH-pi)	L57, I61, I62, F236, F236, F236
5	quinine	10	-7.6	Y239 N92	W88	F236, W88

6	papaverine	10	-7.8	-	F236	W88, I84, I 61
7	chlorpheniramine	10	-7.5	N92	F232, F236	L57, L57, R54, P270
8	benzoin	30	-7.7	Y239	F66, F236, F236	I62
9	parthenolide	30	-7.3	Y239, W88	F66, F236, Y239, W88, W88	-
10	diphenidol	30	-7.9	Y239	F66, F236	I61, I62, W88, K168
11	arborescin	100	-7.5	W88	W88, W88, F236	I62, I69, F236, M243, F66, F236, Y239
12	arglabin	100	-7.6	N92, W88	W88, F236	Y239, F236, F232, F66, I61, L57, W88
13	cascarillin	100	-7.2	N179, K168, W88	W88	F66, G65, L178, M243
14	chloramphenicol	100	-7.3	W88, N92	-	
15	brucine	100	-7.3	W88	-	P72, K168 (multiple)
16	dapsone	100	-7.5	W88, N92, N179	F236	I61
17	cycloheximide	100	-7.6	N92, N92, Y239	Y239, Y239, F236, F232	-
18	Methoxsalen	100	-7.3	N92	-	L57, I61, I62, W88, P270, F236
19	(-) o-Santonin	100	-7.8	N92	-	W88, I61, F236
20	coumarin	300	-6.8	-	-	A99, F232, M96
21	quassin	300	-6.8	K168	-	W88, M166, M243
22	azathioprine	300	-6.5	N92, N92, W88	-	-
23	yohimbine	300	-7.3	-	W88, F236	W88
24	erythromycin	300	-7.4	N175, N179, N179	P72, W88, Y239, Y167	-
25	chloroquine	10000	-6.1	-	W88, F236	G65, F66, I62, L57

The adaptive nature of the TAS2R active site is evident from the different types of binding interactions seen for different ligands, including hydrogen bonding interactions, π-stacking interactions as well as hydrophobic interactions.

Oxygenated tetracyclic triterpenoids like Cucurbitacin E and Cucurbitacin B are among the top-ranking TAS2R10 ligands with an EC_{50} value of 0.01μM. This is in alignment with the results of the docking study with both of these compounds occupying the top two positions in the ranking hierarchy. The molecules make extensive hydrophobic contacts with L57, I61, I62, K168, F236 and P270 as well as hydrogen bonds with N92, Y239 and K256. The binding pose of Cucurbitacin E is shown in Figure 5.

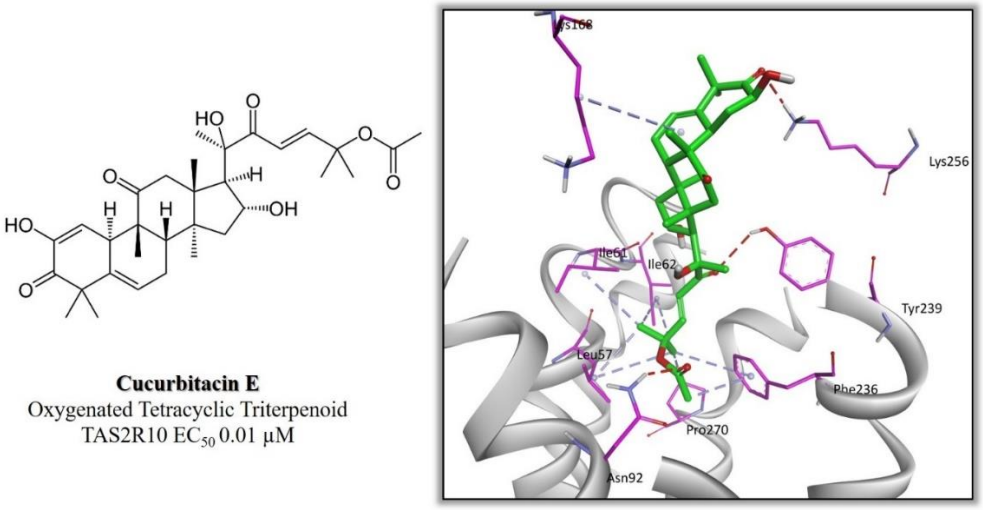

Figure 5: *Left panel* **-** Structure, TAS2R10 EC_{50} value of Cucurbitacin E; *Right panel* - Docked pose of Cucurbitacin E in TAS2R10; TAS2R10 receptor is shown as grey ribbons; TAS2R10 binding site amino acid residues – magenta thin sticks; Cucurbitacin E – thick green sticks; hydrogen bonding interactions – red dashed lines, hydrophobic interactions – grey dashed lines.

Terpene indole alkaloids, strychnine and brucine show differentiation in TAS2R10 binding as is evident in their EC_{50}values of 3 µM and 100 µM respectively, which correlates with the docking scores of -8.3 and -7.3 respectively of their top-raking poses in the homology model of TAS2R10. While strychnine is seen to make numerous deep hydrophobic interactions with L57, I61, I62, F236 (multiple) and a T-π-stack with W88, brucine is seen to get trapped near the extracellular loops due to its ring methoxy groups. The binding pose of strychnine in TAS2R10 and the superimposed poses of brucine with strychnine is shown in the middle and right panel of Figure 6 respectively

.

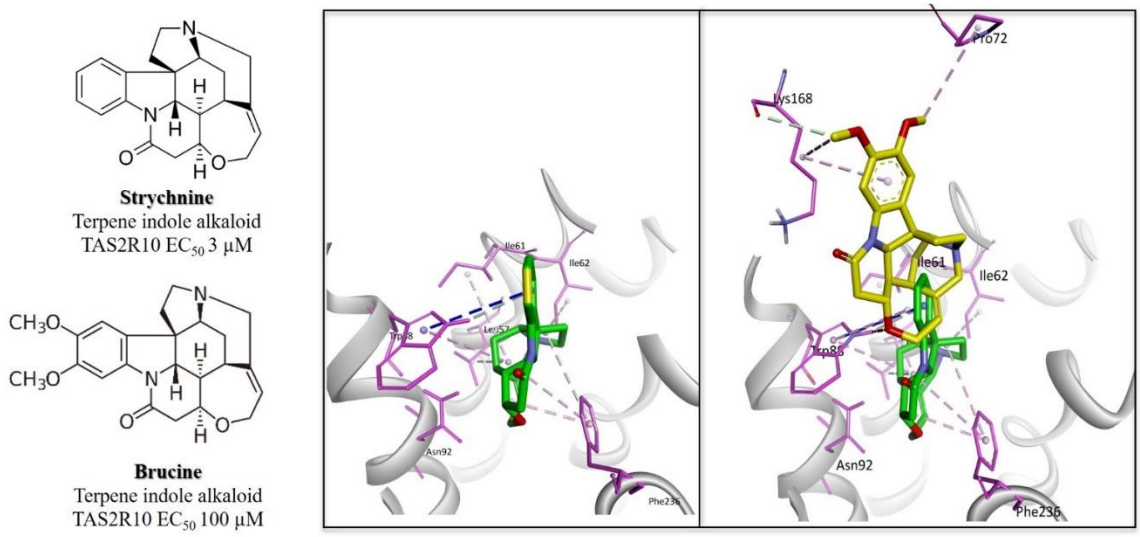

Figure 6: *Left panel*-Structures and TAS2R10 EC_{50} values of Strychnine and Brucine; *Middle panel* - The docked pose of Strychnine (thick green sticks) in TAS2R10; *Right panel* - The superimposed poses of brucine (thick yellow sticks) with strychnine (thick green sticks) in TAS2R10; TAS2R10 receptor is shown as grey ribbons; TAS2R10 binding site amino acid residues – magenta thin sticks; hydrogen bonding interactions – red dashed lines, hydrophobic interactions – grey dashed lines.

Chemically diverse compounds containing two aromatic rings at the molecule termini attached via an appropriate linker such as the quaternary ammonium denatonium, tertiary amine chlorpheniramine, the piperidinyl butanol compound diphenidol and the α-hydroxy ketone molecule benzoin are seen to make two π-stacking interactions with F236 and either F66 or F232. In addition, Denatonium makes a hydrogen bond with N92 via a well-placed central amide linkage and multiple hydrophobic interactions with W88, Y239, M243, I62, which gives it an excellent EC_{50} value of 3 µM. Chlorpheniramine with an EC_{50} value of 10 µM shows one hydrogen bond with N92 and hydrophobic stabilization via amino acids L57, L57, R54, P270. Diphenidol makes a hydrogen bond with Y239 via its tertiary alcoholic group and favourable hydrophobic interactions with I61, I62, and W88 through its long piperidinyl butane subunit. Whereas, benzoin shows a moderately good EC_{50} value of 30 µM. π-stacking interaction of one of the phenyl rings with F236 and a double π-stack of the other phenyl ring with both F66 and F236 contributes significantly towards an EC_{50} value of 30 µM. The docked poses of denatonium, chlorpheniramine, diphenidol and benzoin within TAS2R10 are shown in figure 7.

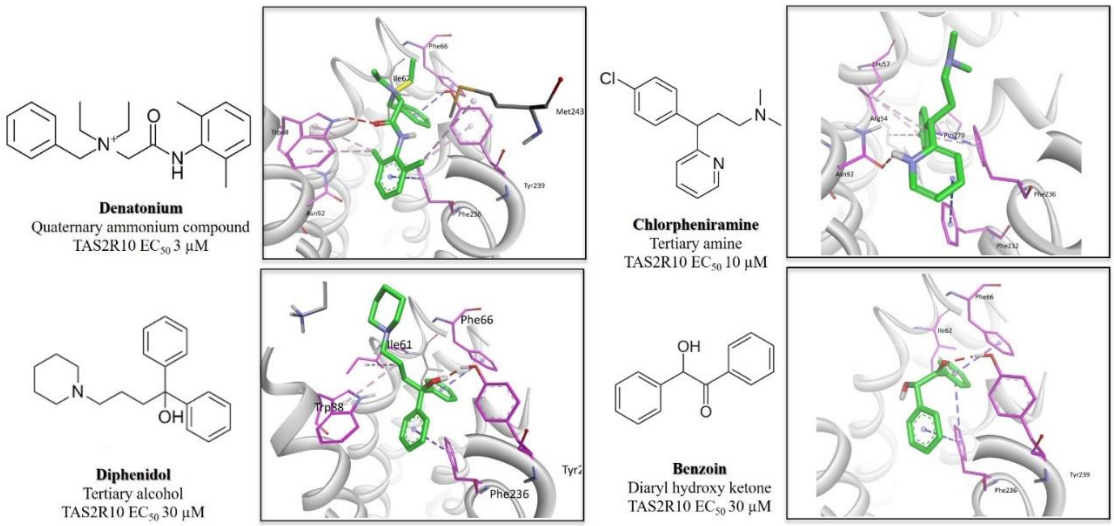

Figure 7: *Top left panel*-Structures, TAS2R10 EC_{50} values and TAS2R10 docked pose of Denatonium (thick green sticks); *Top* right *panel*-Structures, TAS2R10 EC_{50} values and TAS2R10 docked pose of Chlorpheniramine (thick green sticks); *Bottom left panel*-Structures, TAS2R10 EC_{50} values and TAS2R10 docked pose of Diphenidol (thick green sticks);*Bottom right panel*-Structures, TAS2R10 EC_{50} values and TAS2R10 docked pose of Benzoin (thick green

sticks); TAS2R10 receptor is shown as grey ribbons; TAS2R10 binding site amino acid residues – magenta thin sticks; hydrogen bonding interactions – red dashed lines, hydrophobic interactions – grey dashed lines

The quinoline and isoquinoline alkaloids, quinine and papaverine have a TAS2R10 EC_{50} value of 10 µM.

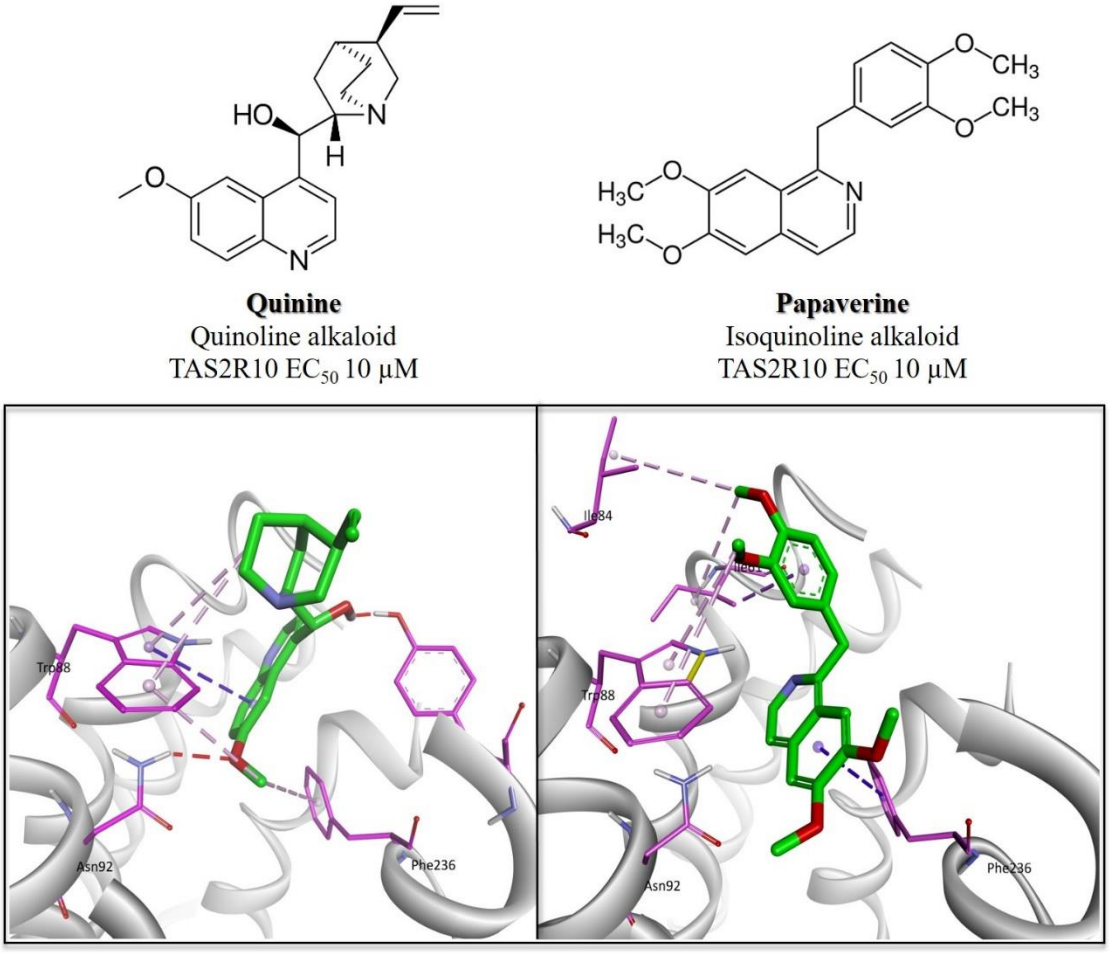

Figure 8: *Left panel*-Structures, TAS2R10 EC_{50} values and TAS2R10 docked pose of Quinine (thick green sticks); *Right panel*-Structures, TAS2R10 EC_{50} values and TAS2R10 docked pose of Papaverine (thick green sticks); TAS2R10 receptor is shown as grey ribbons; TAS2R10 binding site amino acid residues – magenta thin sticks; hydrogen bonding interactions – red dashed lines, hydrophobic interactions – grey dashed lines

Quinine, with a central secondary alcohol makes two hydrogen bonds with Y239 and N92 spanning the binding pocket laterally. F236 anchors the molecule via an interaction with the quinoline methoxy group. The bulky, hydrophobic quinuclidine ring contributes significantly to the binding affinity by forming favourable hydrophobic interactions with W88. Papaverine, with a distinctive lack of hydrogen bond-forming groups has an almost similar docking score as quinine, albeit via several hydrophobic interactions with I61, I84 and W88 and a π-stacking

interaction with F236. The binding poses of quinine and papaverine are shown in figure 8.

Polar molecules like dapsone and cycloheximide have numerous opportunities to from hydrogen bonds within the constraints of the TAS2R10 binding pocket

.

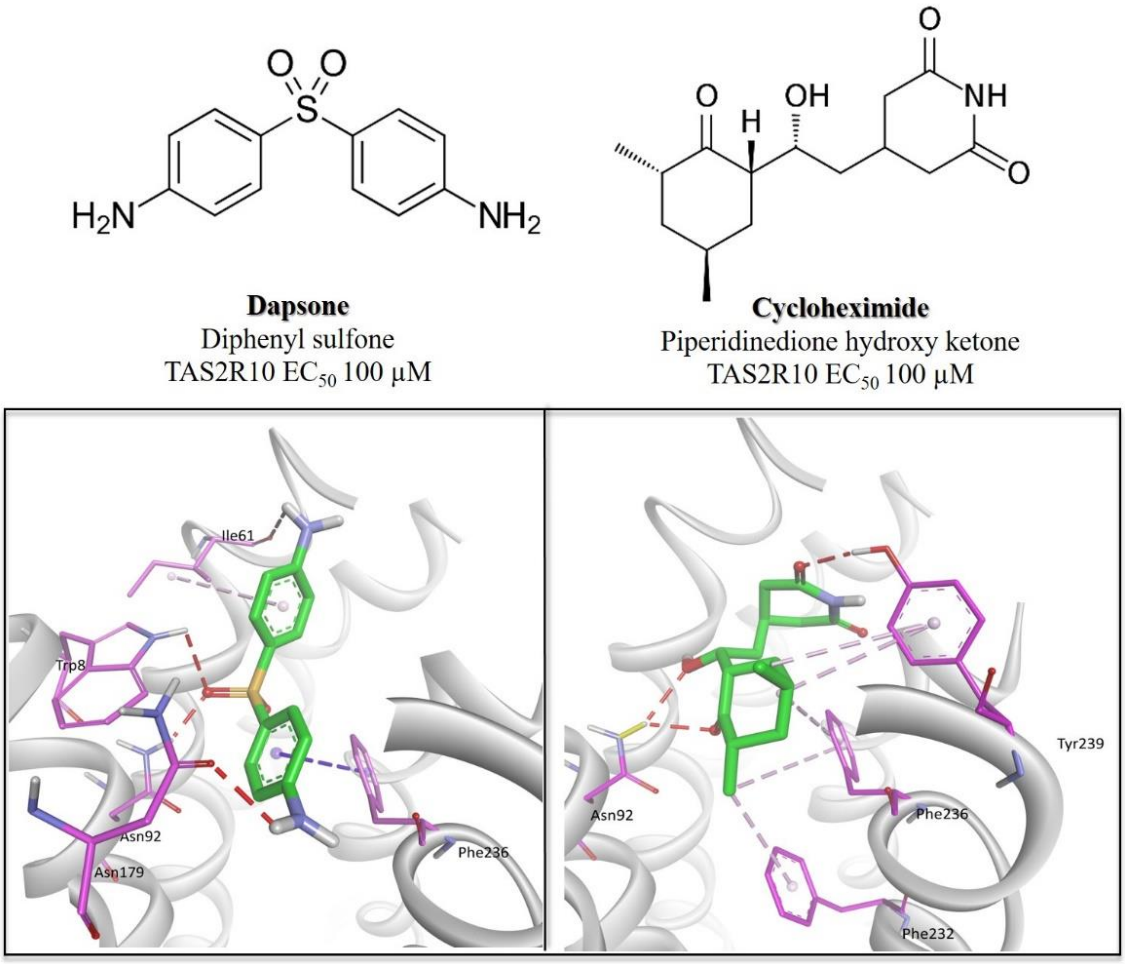

Figure 9: *Left panel*-Structures, TAS2R10 EC_{50} values and TAS2R10 docked pose of Dapsone (thick green sticks); *Right panel*-Structures, TAS2R10 EC_{50} values and TAS2R10 docked pose of Cycloheximide (thick green sticks); TAS2R10 receptor is shown as grey ribbons; TAS2R10 binding site amino acid residues – magenta thin sticks; – Hydrogen bonding interactions – red dashed lines, hydrophobic interactions – grey dashed lines

As seen in figure 9, dapsone forms hydrogen bonds with W88, N92 and N179, whereas cycloheximide shows multiple such interactions with N92 and Y239. However, the predominance of polar binding interactions in these molecules could come at a desolvation penalty cost, which is reflected in their moderate EC_{50}values of 100 µM.

Large, polar molecules have also demonstrated some binding affinity for TAS2R10. Amongst these are the

diterpenoid molecules like cascarillin, the quassinoids (degraded triterpenes) such as quassin and the macrolide antibiotics such as erythromycin. These molecules however, show an alternate binding site residues, which probably prevents them from reaching the deeper, buried amino acids crucial to the activation of TAS2R10. These molecules have moderate binding affinity and docking scores in the TAS2R20 homology model. The superimposed shallow binding of cascarillin, quassin and erythromycin are shown in figure 10.

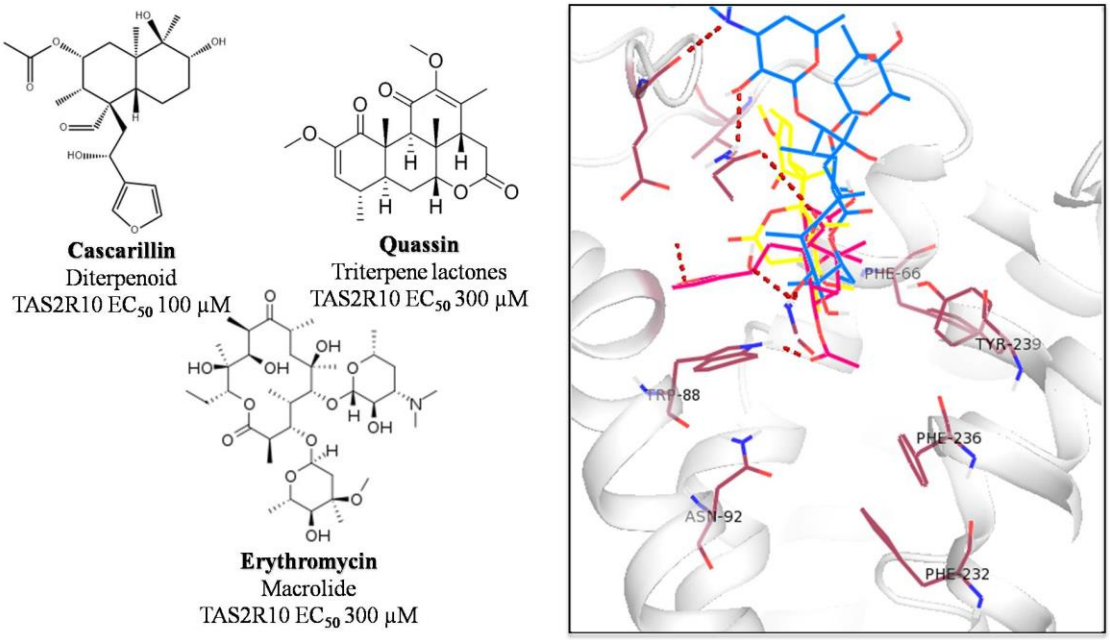

Figure 10: *Left panel*-Structures and TAS2R10 EC_{50} values of Cascarillin, Quassin and Erythromycin; *Right panel* - The superimposed poses of Cascarillin (pink thin lines), Quassin (yellow thin lines) and Erythromycin (cyan thin lines) in TAS2R10; TAS2R10 receptor is shown as grey ribbons; TAS2R10 binding site amino acid residues – magenta thin sticks; hydrogen bonding interactions – red dashed lines.

Thus, the constructed homology model of TAS2R10 provided a rational basis for explaining the promiscuous nature of this bitter taste receptor. The TAS2R binding pocket seems to be endowed with favourable attributes to accommodate compounds with a broad range of sizes, shapes and topologies. The presence of an almost equal proportion of polar and aromatic as well as aliphatic hydrophobic amino acid residues within this pocket nearer to the extracellular loops. The bulky polar compounds make several hydrogen bonding interactions with the superficial amino acid further enables it to house compounds with diverse sets of functional group moieties.

Another interesting artefact of TAS2R10 is the promiscuous nature of its ligands. While several compounds function as ligands for two or three bitter receptors, many of the TAS2R10 modulators such as diphenidol, quinine, chlorpheniramine, denatonium, arborescin, chloramphenicol, azathioprine, cascarillin, arglabin

themselves show good affinity for a host of other bitter receptors with varying degrees of binding affinity. The lack of specific structural motifs for TAS2R10 binding coupled with the profligate nature of its ligands could be indicative of its supplementary role in the bitter receptor family. Mayerhof et al have attributed the existence of promiscuous bitter receptors to the necessity of having compensatory back-up receptors [8] in case of mutation-induced sensory loss. Additionally, the combined affinity of individual compounds to several bitter receptors may be responsible for their intense bitter taste compared to molecules with a narrower range of interacting receptors.

4. Conclusion

Thus, starting from a point of extremely low sequence identity between TAS2R10 and crystallized GPCRs (~11 % sequence identity), we have successfully built a robust homology model of TAS2R10 bitter receptor using single-template homology modelling, induced fit docking of a known bitter reference ligand and long molecular dynamics refinement of the resulting complex. Molecular dynamics simulations, by enabling ligand-induced conformational changes of active site residues provides an excellent alternative for protein structure refinement by exploiting the dynamic nature of proteins. The homology model was validated by docking known TAS2R10 bitter ligands and showed excellent correlation of the docked scores with the experimental EC_{50} values of the ligands. A critical analysis of the docked poses of the TAS2R10 ligands provided insights into the broad spectrum of binding interactions possible for this receptor which was in alignment with its known promiscuous nature.

Acknowledgements

BC would like to thank UGC-SAP, India, for the Research Fellowship. The multiple long molecular dynamics simulations performed on membrane-embedded protein-ligand complexes as part of this work was highly facilitated by the use of Tesla K40 GPU from NVIDIA Corporation. We gratefully acknowledge this donation. The authors would also like to thank Pritesh Bhat and Vinod Devaraji from Schrodinger for their support with the molecular dynamic simulations.

Conflict of Interest

Authors declare no conflicts of interest from a financial or commercial standpoint.

Notes

[a]LigPrep, Schrödinger, LLC, New York, NY, 2017.
[b]PRIME, Schrödinger, LLC, New York, NY, 2017.
[c]Protein preparation wizard, Schrödinger, LLC, New York, NY, 2017.
[d]Desmond, Schrödinger, LLC, New York, NY, 2017.
[e]Site Map, Schrödinger, LLC, New York, NY, 2017.
[f]Induced fit docking, Schrödinger, LLC, New York, NY, 2017.
[g]Glide, Schrödinger, LLC, New York, NY, 2017.

References

[1] B. Lindemann, "Taste reception," *Physiol. Rev.*, vol. 76, no. 3, pp. 719–766, 1996, doi: 10.1152/PHYSREV.1996.76.3.719.

[2] A. Drewnowski and C. Gomez-Carneros, "Bitter taste, phytonutrients, and the consumer: a review," *Am. J. Clin. Nutr.*, vol. 72, no. 6, pp. 1424–1435, 2000, doi: 10.1093/AJCN/72.6.1424.

[3] A. Wiener, M. Shudler, A. Levit, and M. Y. Niv, "BitterDB: a database of bitter compounds," *Nucleic Acids Res.*, vol. 40, no. Database issue, Jan. 2012, doi: 10.1093/NAR/GKR755.

[4] E. Adler, M. A. Hoon, K. L. Mueller, J. Chandrashekar, N. J. P. Ryba, and C. S. Zuker, "A novel family of mammalian taste receptors," *Cell*, vol. 100, no. 6, pp. 693–702, Mar. 2000, doi: 10.1016/S0092-8674(00)80705-9.

[5] S. Soares, E. Brandão, N. Mateus, and V. de Freitas, "Sensorial properties of red wine polyphenols: Astringency and bitterness," *Crit. Rev. Food Sci. Nutr.*, vol. 57, no. 5, pp. 937–948, Mar. 2017, doi: 10.1080/10408398.2014.946468.

[6] H. Matsunami, J. P. Montmayeur, and L. B. Buck, "A family of candidate taste receptors in human and mouse," *Nature*, vol. 404, no. 6778, pp. 601–604, Apr. 2000, doi: 10.1038/35007072.

[7] M. Behrens and W. Meyerhof, "Mammalian bitter taste perception," *Results Probl. Cell Differ.*, vol. 47, pp. 203–220, 2009, doi: 10.1007/400_2008_5.

[8] W. Meyerhof *et al.*, "The Molecular Receptive Ranges of Human TAS2R Bitter Taste Receptors," *Chem. Senses*, vol. 35, no. 2, pp. 157–170, Feb. 2010, doi: 10.1093/CHEMSE/BJP092.

[9] H. D. Belitz and H. Wieser, "Bitter compounds: Occurrence and structure-activity relationships," *http://dx.doi.org/10.1080/87559128509540773*, vol. 1, no. 2, pp. 271–354, Jan. 2009, doi: 10.1080/87559128509540773.

[10] V. DuBois GE, DeSimone, J.A., Lyall, "Chemistry of Gustatory Stimuli," in *The Senses: A comprehensive reference: Olfaction and Taste*, 2008, pp. 27–74.

[11] B. Bufe, T. Hofmann, D. Krautwurst, J. D. Raguse, and W. Meyerhof, "The human TAS2R16 receptor mediates bitter taste in response to beta-glucopyranosides," *Nat. Genet.*, vol. 32, no. 3, pp. 397–401, Nov. 2002, doi: 10.1038/NG1014.

[12] M. Behrens, A. Brockhoff, C. Kuhn, B. Bufe, M. Winnig, and W. Meyerhof, "The human taste receptor hTAS2R14 responds to a variety of different bitter compounds," *Biochem. Biophys. Res. Commun.*, vol. 319, no. 2, pp. 479–485, Jun. 2004, doi: 10.1016/J.BBRC.2004.05.019.

[13] A. Brockhoff, M. Behrens, A. Massarotti, G. Appending, and W. Meyerhof, "Broad tuning of the human bitter taste receptor hTAS2R46 to various sesquiterpene

lactones, clerodane and labdane diterpenoids, strychnine, and denatonium," *J. Agric. Food Chem.*, vol. 55, no. 15, pp. 6236–6243, Jul. 2007, doi: 10.1021/JF070503P.

[14] S. Born, A. Levit, M. Y. Niv, W. Meyerhof, and M. Behrens, "The Human Bitter Taste Receptor TAS2R10 Is Tailored to Accommodate Numerous Diverse Ligands," *J. Neurosci.*, vol. 33, no. 1, p. 201, Jan. 2013, doi: 10.1523/JNEUROSCI.3248-12.2013.

[15] S. Rodgers, J. Busch, H. Peters, and E. Christ-Hazelhof, "Building a tree of knowledge: analysis of bitter molecules," *Chem. Senses*, vol. 30, no. 7, pp. 547–557, Sep. 2005, doi: 10.1093/CHEMSE/BJI048.

[16] C. Cervellati *et al.*, "A qNMR approach for bitterness phenotyping and QTL identification in an F1 apricot progeny," *J. Biotechnol.*, vol. 159, no. 4, pp. 312–319, Jun. 2012, doi: 10.1016/J.JBIOTEC.2011.09.004.

[17] A. N. Pronin, H. Tang, J. Connor, and W. Keung, "Identification of ligands for two human bitter T2R receptors," *Chem. Senses*, vol. 29, no. 7, pp. 583–593, 2004, doi: 10.1093/CHEMSE/BJH064.

[18] UniProt, "The universal protein knowledgebase.," *Nucleic Acids Res.*, vol. 45, no. D1, pp. D158–D169, 2017.

[19] R. A. Laskowski, M. W. MacArthur, D. S. Moss, and J. M. Thornton, "PROCHECK: a program to check the stereochemical quality of protein structures," *J. Appl. Crystallogr.*, vol. 26, no. 2, pp. 283–291, Apr. 1993, doi: 10.1107/S0021889892009944.

[20] M. Wiederstein and M. J. Sippl, "ProSA-web: interactive web service for the recognition of errors in three-dimensional structures of proteins," *Nucleic Acids Res.*, vol. 35, no. suppl_2, pp. W407–W410, Jul. 2007, doi: 10.1093/NAR/GKM290.

[21] M. J. Sippl, "Recognition of errors in three-dimensional structures of proteins," *Proteins Struct. Funct. Bioinforma.*, vol. 17, no. 4, pp. 355–362, Dec. 1993, doi: 10.1002/PROT.340170404.

[22] J. Sivakamavalli, S. K. Tripathi, S. K. Singh, and B. Vaseeharan, "Homology modeling, molecular dynamics, and docking studies of pattern-recognition transmembrane protein-lipopolysaccharide and β-1,3 glucan-binding protein from Fenneropenaeus indicus," *J. Biomol. Struct. Dyn.*, vol. 33, no. 6, pp. 1269–1280, 2015, doi: 10.1080/07391102.2014.943807.

[23] I. G. Tikhonova, B. Selvam, A. Ivetac, J. Wereszczynski, and J. A. McCammon, "Simulations of Biased Agonists in the β2 Adrenergic Receptor with Accelerated Molecular Dynamics," *Biochemistry*, vol. 52, no. 33, p. 5593, Aug. 2013, doi: 10.1021/BI400499N.

[24] H. Ioannidis *et al.*, "Alchemical Free Energy Calculations and Isothermal Titration Calorimetry Measurements of Aminoadamantanes Bound to the Closed State of Influenza A/M2TM," *J. Chem. Inf. Model.*, vol. 56, no. 5, pp.

862–876, May 2016, doi: 10.1021/ACS.JCIM.6B00079.

[25] Y. Jiang, J. Zou, and C. Gui, “Study of a ligand complexed with Cdk2/Cdk4 by computer simulation,” *J. Mol. Model.*, vol. 11, no. 6, pp. 509–515, Nov. 2005, doi: 10.1007/S00894-005-0263-8.

[26] A. Dagan-Wiener *et al.*, “BitterDB: taste ligands and receptors database in 2019,” *Nucleic Acids Res.*, vol. 47, no. Database issue, p. D1179, Jan. 2019, doi: 10.1093/NAR/GKY974.

[27] S. Kim *et al.*, “PubChem in 2021: new data content and improved web interfaces,” *Nucleic Acids Res.*, vol. 49, no. D1, pp. D1388–D1395, Jan. 2021, doi: 10.1093/NAR/GKAA971.

[28] N. M. O’Boyle, M. Banck, C. A. James, C. Morley, T. Vandermeersch, and G. R. Hutchison, “Open Babel: An Open chemical toolbox,” *J. Cheminform.*, vol. 3, no. 10, pp. 1–14, Oct. 2011, doi: 10.1186/1758-2946-3-33/TABLES/2.

[29] S. Dallakyan and A. J. Olson, “Small-molecule library screening by docking with PyRx,” *Methods Mol. Biol.*, vol. 1263, pp. 243–250, 2015, doi: 10.1007/978-1-4939-2269-7_19.

[30] BIOVIA, *Dassault Systèmes, Discovery Studio Visualizer*. 2021.